Journal of Colloid and Interface Science 344 (2010) 395–401

Contents lists available at ScienceDirect

Journal of Colloid and Interface Science

www.elsevier.com/locate/jcis

Electrical and optical percolations of polystyrene latex–multiwalled carbon nanotube composites

Selim Kara [a,*], Ertan Arda [a], Fahrettin Dolastir [a], Önder Pekcan [b]

[a] Department of Physics, Trakya University, 22030 Edirne, Turkey
[b] Kadir Has University, Cibali, 34083 Istanbul, Turkey

ARTICLE INFO

Article history:
Received 29 July 2009
Accepted 31 December 2009
Available online 11 January 2010

Keywords:
PS–MWCNT composite
Percolation threshold
Electrical conductivity

ABSTRACT

Electrical conductivity and optical transmittance properties of polystyrene (PS)–multiwalled carbon nanotube (MWCNT) composite films were investigated. Composite films were prepared by mixing of various mass fractions of MWCNT in PS–water dispersions. After water evaporates, powder composite films were annealed at 175 °C above the glass transition of PS for 20 min. Photon transmission and two point probe resistivity techniques were employed to determine the variations of the optical and the electrical properties of composites. Transmitted light intensity, I_{tr} and surface resistivity, R_s were monitored as a function of MWCNT mass fraction (M). It was observed that, both the surface resistivity and the optical transparency were decreased by increasing the amount of MWCNT added to the polymeric system. Conductivity and optical results were interpreted according to the classical and site percolation theory, respectively. The electrical (σ) and the optical (op) percolation threshold values and critical exponents were calculated as $M_\sigma = 1.8$ wt.%, $M_{op} = 0$–0.13 wt.% and $\beta_\sigma = 2.25$, $\beta_{op} = 0.32$, respectively.

1. Introduction

Polymer–carbon nanotube (CNT) composites were first reported by Ajayan et al. after the carbon nanotubes has discovered by Iijima [1]. Recently, carbon nanotubes and their polymer-composites are used in various industrial areas such as flat panel screens, electron microscope guns, gas discharge tubes, microwave amplifiers, fuel cells, batteries, hydrogen storing media, nanoprobes, sensors and body-parts of aircrafts and spacecrafts [2]. Some CNTs are stronger than steel and lighter than aluminum and more conductive than copper [2]. Thus, studies on polymer–CNT composites have been accelerated at last decade.

There are two main types of CNT known as single (SWCNT) and multiwalled (MWCNT). Thermoplastic polymers are usually used as an insulating material because of their low electrical conductivity properties ($\approx 10^{-15}$ S/m). Dispersing the conducting filler such as carbon black and CNT in polymer phase forms conductive polymer-composites. Electrical resistivities of polymer–MWCNT composites which are strongly dependent on the volume or mass fractions of the CNTs may vary between 10^{16} to several ohms. At low volume or mass fractions, the resistivity remains very close to the resistivity of pure polymer. Insulating polymers are transformed to conductive composites by addition of CNTs above a critical concentration threshold (known as percolation threshold). When the positions of CNTs in the polymer matrix form a conducting network, the conductivity of composite sharply increases. This phenomenon is known as percolation and can be well explained by percolation theory [3]. Percolation threshold can be determined by measuring the resistivity variations in composites. Electrical percolation thresholds for some MWCNT and SWCNT polymer-composites were reported as ranging from 0.0021 to 15 wt.% [4]. Studies on polymer–CNT composites show that their electrical, mechanical and thermal properties are improved by addition of CNTs [5–9].

PS–MWCNT composites have been widely studied and published in the literature. The results of Yu et al. yield an increment in conductivities of such composites which were produced by latex technology [10]. They measured percolation threshold, φ_c of the composites by 4-probe electrical measurement technique and found to be 1.5 wt.%. Furthermore, effects of different sodium dodecyl sulfate (SDS) concentrations on the composite conductivities were also investigated [10]. The similar composite structures which were produced by the same techniques were studied by Wu and Chen [11]. They determined that conductivity, mechanical properties and T_g from DSC data of composite systems which were increased by addition of MWCNT [11]. Grossiord et al. showed that conductivities and percolation thresholds of composites which were prepared by compression molding technique were affected by process time and temperature [12]. Besides electrical conductivities, thermal and mechanical properties such as elastic modulus of composites were observed to be increased by increasing concentration of nanotube [13–16]. Similar studies were performed for PS–SWCNT composites. It was observed that electrical, thermal and mechanical properties of the composites were highly improved [9,17,18].

* Corresponding author. Fax: +90 284 235 11 98.
E-mail address: skara@trakya.edu.tr (S. Kara).

0021-9797/$ - see front matter © 2010 Elsevier Inc. All rights reserved.
doi:10.1016/j.jcis.2009.12.056

Effects of molecular weight, annealing time and temperature, solvent type, film thickness on film formation from hard and soft latex particles such as Poly(methyl methacrylate) (PMMA), Poly(vinyl acetate) (PVAc) and PS were studied using photon transmission technique by our group [19–21]. In this work, the effect of MWCNT addition in insulating PS matrix was investigated. Variations in electrical and optical properties of very-thin PS–MWCNT composite films were measured by using 2-probe resistivity measurement and photon transmission techniques. Electrical and optical percolation thresholds were determined. Classical and site percolation theories were used to calculate the critical exponents for conductivity and optical transmission data, respectively. Percolation thresholds and critical exponents for optical and electrical data were found to be different, depending on the applied percolation model.

2. Materials and methods

2.1. Multiwalled carbon nanotubes (MWCNT) and polystyrene (PS) latexes

MWCNT (Aldrich 659258) with outer diameter of 110–170 nm and length of 5–9 μm was purchased and used as it is to prepare the composites. Poly(vinyl pyrrolidone) (PVP40, Sigma–Aldrich) was used as dispersion agent for MWCNTs in water.

The monomer, styrene (S) (Yarpet A.S., Turkey), was treated with aqueous NaOH to remove the inhibitor and stored in a refrigerator until use. The initiator was 2,2-azobis(isobutyronitrile) (AIBN, BDH Chemicals Ltd., UK). Ethyl alcohol (Merck, Germany)–water mixtures were used as the dispersion medium. Poly(vinyl pyrrolidone) (PVP) (30K, Fluka, Switzerland) was used as a steric stabilizer. Polymerizations were carried out in a magnetically driven, sealed, cylindrical reactor equipped with a temperature-control system [22,23]. One gram of PVP was dissolved in a dispersion medium containing 90 mL of ethyl alcohol and 10 mL of water. The monomer phase was prepared by dissolving 140 mg in 10 mL of styrene. Two phases were mixed and charged to a reactor agitated with an anchor-type agitator at a speed of 150 rpm, and the polymerization was conducted at 80 °C for 24 h. The PS latex obtained was cleaned by using the serum replacement and ion-exchange methods described previously [22,23]. The average particle size of PS particles was evaluated using scanning electron micrographs and the average size of the PS particles was found 2 μm. The average molecular weight of PS particles was determined by a HPLC system (Waters, USA). The GPC unit, consisting of a Waters Model 510 HPLC pump and a Waters U6K injector, was equipped with two Ultrastyragel columns (Waters, 10 and 500 Å) in series and a Waters 486 tunable absorbance detector. Chloroform was used as both the solvent and the eluent. Elution was performed at 30 °C and a flow rate of 1 mL/min, using a Waters 510 HPLC pump. The columns were calibrated with polystyrene standards (Shodex Standards, SL-105, Showa Denko, Japan). Molecular weight of PS particles was found to be 3.6×10^4 g/mol.

2.2. Composite film preparation

Van der Waals forces between the MWCNTs prevent them to form homogeneous distribution in water. Generally dispersing agents such as PVP, SDS and tetrahydrofuran (THF) or sonication technique are used. PS (3.5% w/v)–MWCNT dispersion in water was prepared by using a magnetic stirrer for 24 h. PVP was added to this dispersion with a concentration of 5 mg/mL to separate the MWCNTs from each other. The final dispersion was splitted into 17 different containers, each of with different MWCNT concentrations. A pure PS (non MWCNT content) dispersion was also prepared as a standard. Mass fractions of PS–MWCNT dispersions were calculated from the following relation

$$M = \frac{m_{\mathrm{MWCNT}}}{m_{\mathrm{MWCNT}} + m_{\mathrm{PS}}} \tag{1}$$

where m_{MWCNT} and m_{PS} are the masses of the MWCNT and PS in the dispersions, respectively. Calculated mass fractions by using Eq. (1) are: 0 (pure PS), 0.13, 0.4, 0.6, 0.9, 1.2, 1.5, 1.8, 2.2, 2.75, 3.4, 3.9, 4.5, 6.0, 8.5, 14 and 18 wt.%, respectively. Composite films were prepared from PS–MWCNT dispersions on 2.5×3.0 cm^2 glass plates by using micropipette, then allowing the water to evaporate at room temperature. We were careful to ensure that the liquid

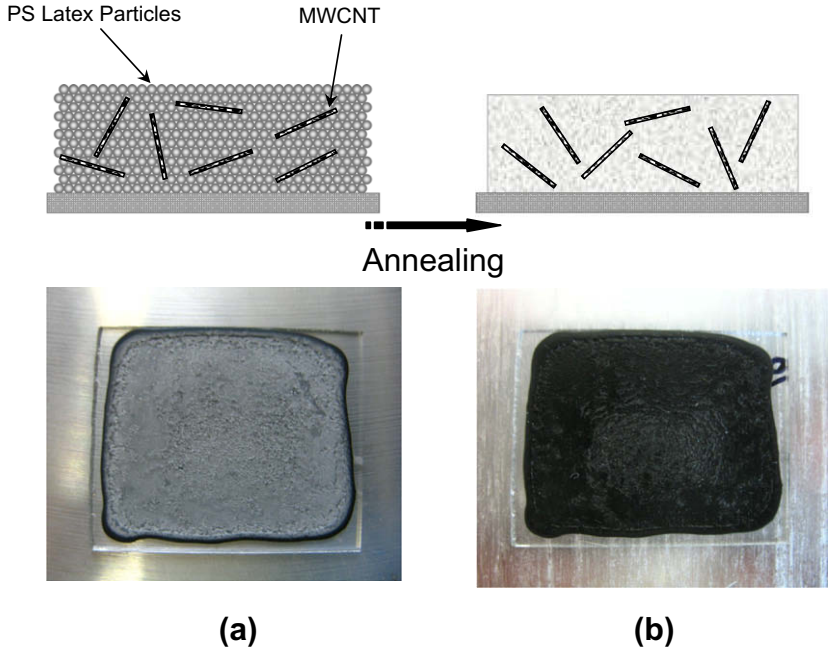

Fig. 1. Photographs of the film with 3.4 wt.% mass fraction and cartoon representations of film cross-section: (a) before and (b) after the annealing process.

dispersion from the droplets covered the whole surface area of the plate and remained there until the water evaporated. Samples were weighed before and after the film casting to determine the film thicknesses. The average film thickness was determined as 34 μm. After the water evaporation, all the composite films were annealed at 175 °C above the glass transition of PS for 20 min at room conditions to complete the film formation process [20,24] before the resistivity and photon transmission measurements were performed. Fig. 1 shows the composite film with 3.4 wt.% mass fraction of MWCNT, and cartoon representations of film cross-section: (a) before and (b) after the annealing process.

2.3. Optical transmission and resistivity measurements

After the annealing process was completed, each composite film was placed in a UVV spectrophotometer (Lambda 2S of Perkin–Elmer, USA) and their transmittance were detected at 400 nm wavelength. Measurements were performed at six different positions on the film surface to lower the error level, and so the average value of transmitted light intensity was obtained. All the photon transmission measurements were carried out at room temperature.

Electrical resistivities of the composite films were measured by alternating polarity technique with Keithley Model 6517A electrometer which employs the ASTM D-257 measurement method, and a test fixture which was reconstructed as three times minimized version of Keithley Model 8009 resistivity test fixture. The composite films were placed in the text fixture which have disk shaped electrodes, then their surface resistivities, R_s (Ohm/square or Ohm) were measured under 100 V DC potential with alternating polarities for every 15 s periods. All the resistivities of the composite films were determined for four different orientations and measurements were repeated for many times to lower the error level. The average values obtained from the stable measurements were used to plot the graphics. A photograph of the test fixture and some technical drawings about surface resistivity measurements are presented in Fig. 2.

3. Results and discussion

3.1. Electrical percolation

The variation in the surface resistivities (R_s) of PS–MWCNT composite films versus mass fractions (M) of MWCNT are shown in Fig. 3. One can see from the Fig. 3 that surface resistivities (R_s) of the composite films do not change apparently up to $M \leqslant 1.8$ wt.%. However, surface resistivities of the composite films dramatically decrease from $10^{12}\,\Omega$ to $10^{6}\,\Omega$ in the band-gap of $M = 1.8$–4.0 wt.%. This behavior indicates that the percolation occurs at low levels of M.

The conductivity values are calculated from the following equation,

$$\sigma = 1/R_s \tag{2}$$

then, the produced results from Eq. (2) are presented in Fig. 4. It can be seen from Fig. 4 that, the conductivity, σ dramatically increases above $M_\sigma = 1.8$ wt.% by the addition of small amount of MWCNT into the insulating PS matrix. This tendency of increase can be interpreted by the existence of vertical conductive paths of MWCNTs in the composite film.

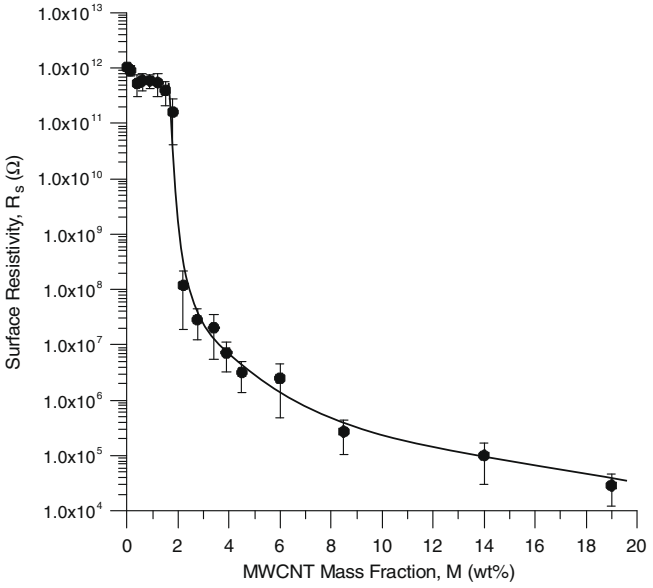

Fig. 3. Surface resistivities of the PS–MWCNT composite films versus mass fractions.

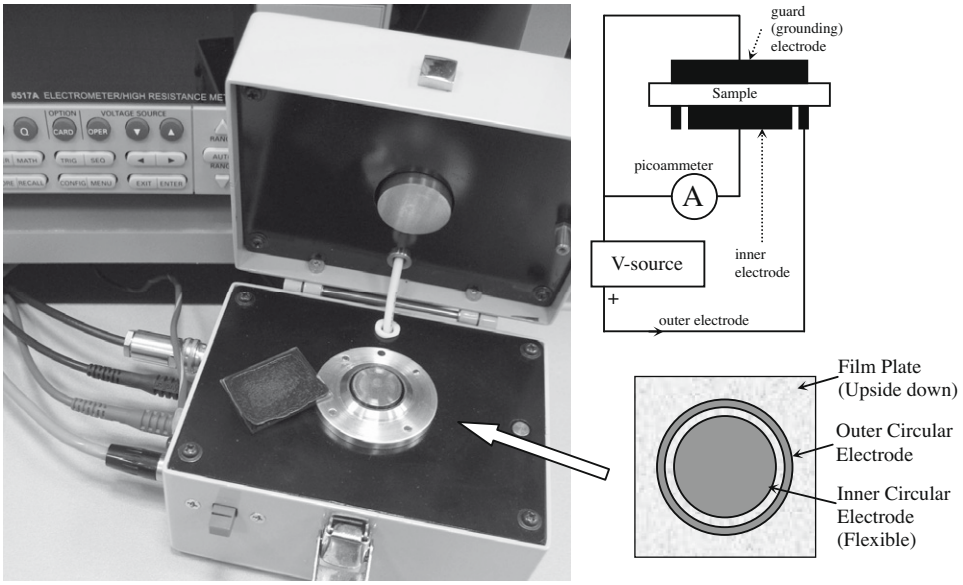

Fig. 2. Photograph of the test fixture and its working principle.

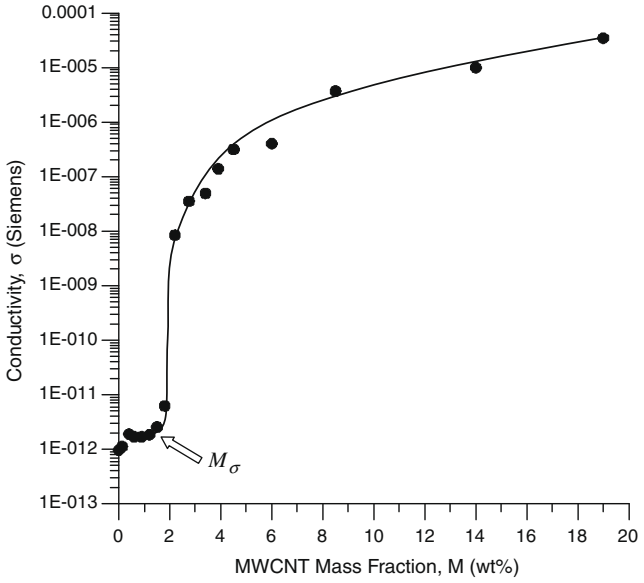

Fig. 4. Variation in the conductivities, σ which were calculated by Eq. (2) versus mass fractions.

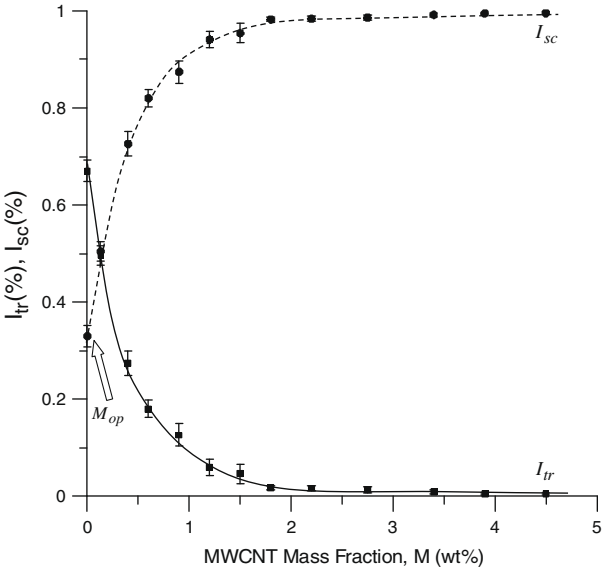

Fig. 6. Variation in transmitted (I_{tr}) and scattered (I_{sc}) light intensities on PS–MWCNT composite films versus mass fractions.

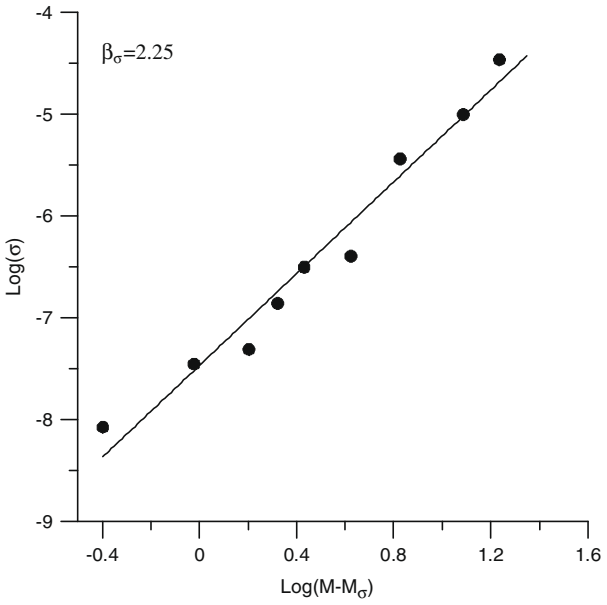

Fig. 5. Logarithms of conductivities versus $(M - M_\sigma)$ values. The slope of the fit gives the critical exponent, β_σ for electrical percolation according to Eq. (3).

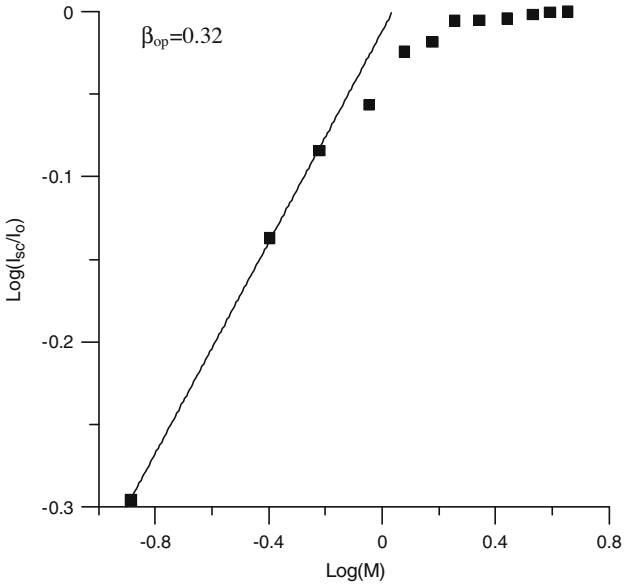

Fig. 7. The variation of $\log(I_{sc}/I_o)$ versus $\log(M)$.

Thus, the insulating system, at this point starts to transform to a more conductive state, which indicates that the percolation threshold of conductivity (M_σ) is 1.8 wt.%. According to classical percolation theory, one can use the following equation for a dilute ($M > M_\sigma$) composite structure [3].

$$\sigma = \sigma_o (M - M_\sigma)^{\beta_\sigma} \tag{3}$$

where M is the volume or mass fraction of MWCNT, σ is the conductivity (Siemens), M_σ is the percolation threshold value, β_σ is the critical exponent for the conductivity and σ_o is the conductivity of pure MWCNT film. β_σ was calculated and found to be 2.25 from the slope of the $\log\sigma - \log(M - M_\sigma)$ plot in Fig. 5 which was fitted to a perfectly straight line.

In literature, the calculated theoretical critical exponents in 3D network systems are in between 1.6 and 2.0 and experimentally obtained β_σ values vary in between 1.3 and 3.1 [25]. The $\beta_\sigma = 2.25$ value produced in this work is well agreed with the theoretical and the experimental data in the literature. In an experimental study for PS–MWCNT composites, performed by Kota et al., the critical exponents were found as 1.5 and 1.9 for the solvents of dimethyl formamide (DMF) and THF, respectively. The corresponding percolation thresholds for volume fraction were found as 0.019 and 0.017 for the same solvents [26]. Blighe et al. experimentally found β_σ as 2.2 ± 0.2 for PS–SWCNT system [17]. For a similar system, the critical percolation threshold point was determined as 0.25% (volumetric) by Andrews et al. [27]. The different β_σ values are related to micro-structural properties (i.e. CNT size, film thickness etc.) of PS–CNT composites.

3.2. Optical percolation

Both the transmitted (I_{tr}) and scattered (I_{sc}) light intensities versus mass fractions of composite films are given in Fig. 6, where it can be seen that transmitted light intensity, I_{tr} from the composite films sharply decrease as M increases. Additionally, there is almost no light transmission from the films above $M \geqslant 2.0$ wt.%. The decrease in the level of I_{tr} can be explained by the interpenetration

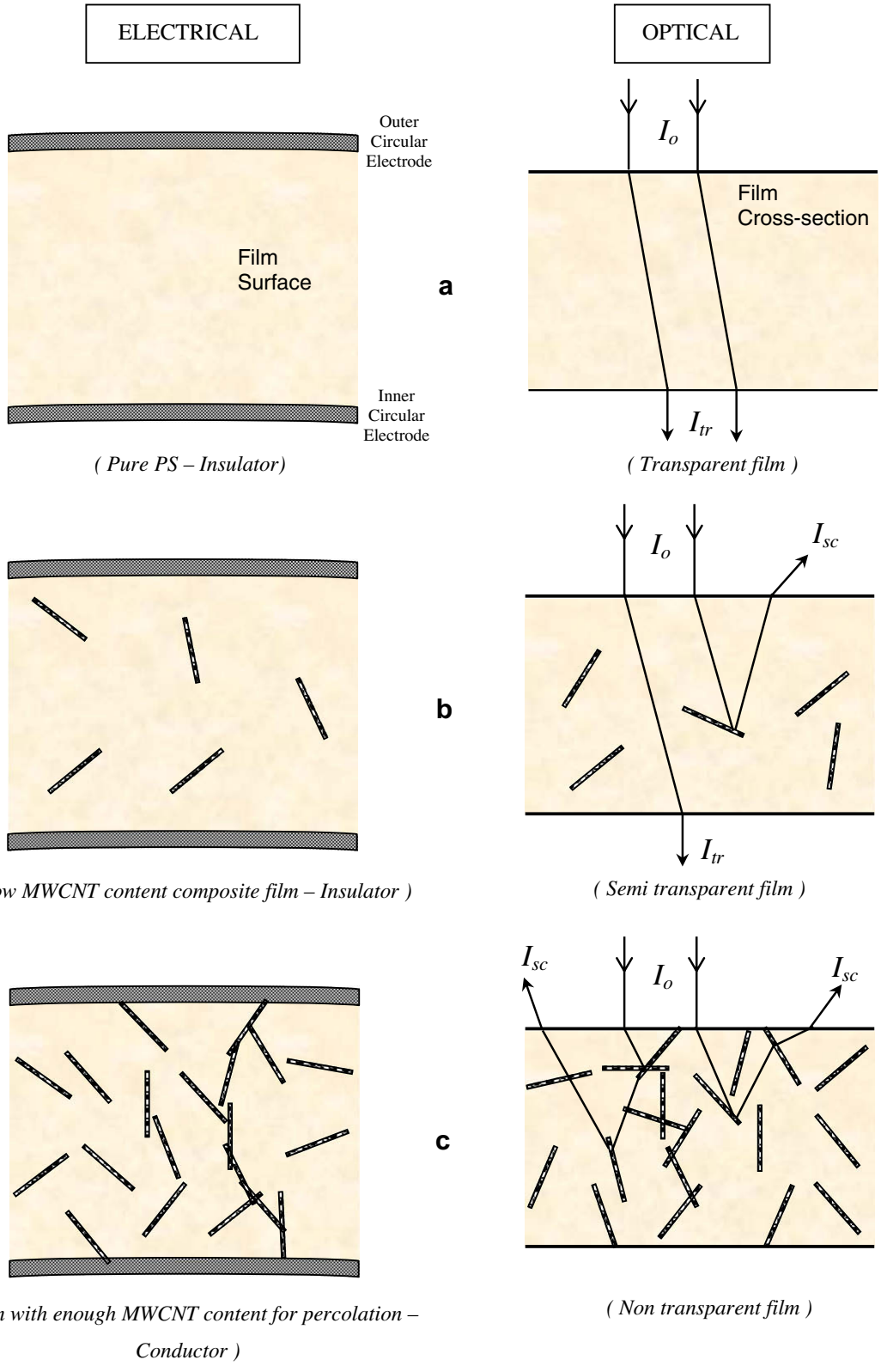

Fig. 8. Cartoon representation of the difference between optical and electrical percolations for: (a) pure PS (non MWCNT) film, (b) low MWCNT content composite film, and (c) composite film with high enough MWCNT content to pass the electrical percolation threshold.

of MWCNTs among the homogeneously dispersed PS chains, i.e. two medium with different refractive indices are randomly formed in the composite system. Scattering centers in the film are increased as M is increased. Thus, more light is scattered and, as a result, optical transmission of films is decreased.

The obtained optical transmission data can be treated by the site percolation theory where sites in a lattice are either filled or empty. Extended simulations and theoretical works have shown that the percolation probability is given as

$$P_\infty(p) \propto (p - p_c)^\beta \tag{4}$$

If we assume that the M in Fig. 6 is identical to lattice occupation probability, p, then the percolation threshold value, p_c will be equivalent to M_{op}. One can arrange the percolation equation (Eq. (4)) for the optical data as

$$I_{sc}(M) = I_o(M - M_{op})^{\beta_{op}} \tag{5}$$

by assuming that the percolation probability ($P_\infty(p)$) is proportional to scattered light intensity $I_{sc} = 1 - I_{tr}$. Eq. (5) represents the percolation model for the MWCNT distribution in the PS matrix. Here, M represents the lattice occupation probability of MWCNTs in the PS matrix and M_{op} is the critical threshold of M. As M is increased, the scattered light intensity, I_{sc} increases due to the concentration fluctuations. In Fig. 6, the scattered light intensity increases rapidly, even though the MWCNT content was 0.13 wt.% at the beginning which shows the percolation threshold value is in between 0 and 0.13 wt.%. Since $M - M_{op} \to M$ for the extremely low M_{op} values, the Eq. (5) can be written as

$$I_{sc}(M) = I_o M^{\beta_{op}} \tag{6}$$

The variation of $\log I_{sc}/I_o$ versus $\log(M)$ is given in Fig. 7. The critical exponent, β_{op} was calculated and found to be as 0.32 from the slope of the straight line in Fig. 7, according to Eq. (6). The obtained value of $\beta_{op} = 0.32$ is not far from the theoretical site percolation value of 0.42 [3]. The difference may be originated from the conditions of sample preparation and measurement. In current work, the threshold and the critical exponent values of electrical percolation were found to be higher than that of optical percolation.

This difference has similarities quite parallel with other experimental studies. Previous experimental studies for some conductive polymeric composites have shown that rheological percolation threshold was lower than the electrical percolation threshold. Du et al. determined the electrical and rheological percolation threshold values for PMMA–SWNT composite as $m_{c\sigma} = 0.39$ and $m_{cG'} = 0.12\%$, respectively. Furthermore, they found the critical exponents for the electrical and rheological measurements as $\beta_\sigma = 2.3$ and $\beta_{G'} = 0.7$, respectively [7]. In another experimental study performed by using electrical, viscosity and modulus measurement techniques on PET–MWCNT composite system, the percolation thresholds and the critical exponents were found as $m_{c,\sigma} = 0.009$, $m_{c,\eta} = 0.006$, $m_{c,G'} = 0.005$ and $\beta_{c,\sigma} = 2.2$, $\beta_{c,\eta} = 1.3$, $\beta_{c,G'} = 1.5$, respectively [28].

In Fig. 8, the difference between optical and electrical percolations is represented by a picture which describes the process. Fig. 8a shows the optical and electrical behavior of the pure PS film. The conductivity is extremely low and the optical transmittance is quite high for this film. Fig. 8b represents the optical and electrical behavior for films with low MWCNT. While the optical transmittance is decreased due to the existence of MWCNTs (existence of different refractive mediums), the scattered light intensity increases. Since the electrical conductivity increases under the certain conditions such as formation of vertical conductive paths (between CNTs or electron tunneling) the electrical conductivity is still at the same initial level. The tunneling range between CNTs must be lower than 5 nm [7]. After the electrical percolation threshold, the composite system seems like in Fig. 8c. The CNTs form a certain number of vertical conductive paths and as a result, the electrical conductivity is increased. However, the composite film scatters high number of photons due to increase in the heterogeneity level of the film.

The obtained data by the both systems are given together in Fig. 9 for comparison. As one can see in Fig. 9, the electrical percolation starts at the saturation level of the optical percolation. This behavior accords with the model presented in Fig. 8.

4. Summary

This article has shown that the insulator–conductor transition takes place by addition of a small amount of MWCNT in the PS–MWCNT composite system. The electrical percolation starts at the mass fraction of 1.8 wt.% and is almost accomplished at the mass fraction of 8.0 wt.%. It was found that optical percolation process for polymer–CNT thin film composites can also be observed by using optical transmission technique. Nevertheless, both the observed electrical and optical percolation threshold values are different from each other. Electrical and optical percolation parameters such as percolation thresholds and critical exponents were obtained in accordance with the classical and site percolation theories, respectively. Our results for the electrical percolation are well agreed with the experimental data which were obtained by other groups for PS–MWCNT composite system.

The most important finding of this work is the low percolation threshold (around 0.1%) of the optical transparency, which is usually known to be around 0.25 in 3D systems [29–32]. Here, however, opaqueness starts to percolate quite early by predicting similar behavior of electrical conductivity in the composite. It is easy to understand the early threshold of conductivity due to hopping and/or tunneling of electrons in CNT–polymer composite. However, early percolation of opaqueness is in question, most probably the nano-size of CNT plays a fundamental role for the scattering of light from the composite film. In other words, inclusion of very small amount of CNT scatters light dramatically, similar to the sudden increase of electrical conductivity.

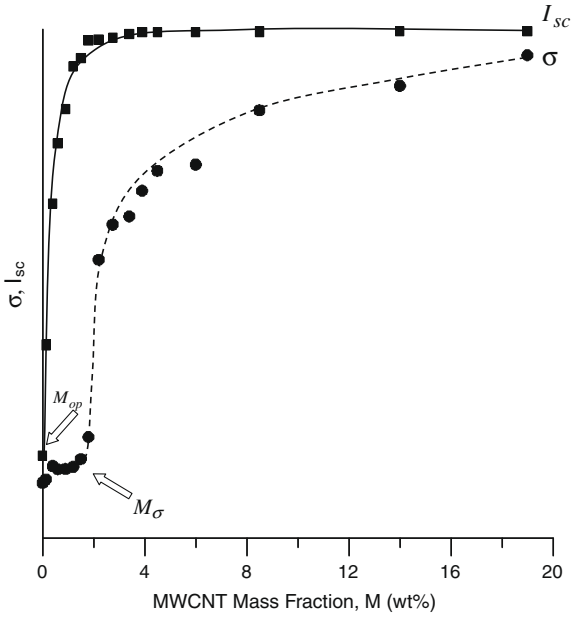

Fig. 9. Comparison of scattered light intensities, I_{sc} and conductivities, σ versus mass fractions.

The other important out come from this work is finding the electrical percolation threshold at the point where optical transparency has completely disappeared, i.e. lost of optical transparency results the beginning of electrical conductivity, which increases and saturates in totally opaque composite film. This behavior may bring some industrial predictions in applied areas, such as electron hopping and/or tunneling is able to start after complete opaqueness has been reached, i.e. transparent CNT–polymer film cannot percolate conductivity. As a result, in applied areas testing of opaqueness of the CNT–polymer film may predict their conductive behavior.

Acknowledgments

The authors thank to Professor Erhan Piskin for providing PS particles and Trakya University-Bilimsel Arastirma Projeleri Birimi (TUBAP) for their financial support.

References

[1] M. Moniruzzaman, K.I. Winey, Macromolecules 39 (2006) 5194.
[2] P.M. Ajayan, O.Z. Zhou, Top. Appl. Phys. 80 (2001) 391.
[3] D. Stauffer, A. Aharony, Introduction to Percolation Theory, Taylor & Francis, London, 1994.
[4] W. Bauhofer, J.Z. Kovacs, Compos. Sci. Technol. 69 (2009) 1486.
[5] L. Gao, X. Zhaou, Y. Ding, Chem. Phys. Lett. 434 (2007) 297.
[6] C.S. Choi, B.J. Park, H.J. Choi, Diamond Relat. Mater. 16 (2007) 1170.
[7] F. Du, R.C. Scogna, W. Zhou, S. Brand, J.E. Fischer, K.I. Winey, Macromolecules 37 (2004) 9048.
[8] S.J. Park, S.T. Lim, M.S. Cho, H.M. Kim, J. Joo, H.J. Choi, Curr. Appl. Phys. 5 (2007) 302.
[9] T.E. Chang, A. Kisliuk, S.M. Rhodes, W.J. Brittain, A.P. Sokolov, Polymer 47 (2006) 7740.
[10] J. Yu, K. Lu, E. Sourty, N. Grossiord, C.E. Koning, J. Loos, Carbon 45 (2007) 2897.
[11] T.M. Wu, E.C. Chen, Compos. Sci. Technol. 68 (2008) 2254.
[12] N. Grossiord, P.J.J. Kivit, J. Loos, J. Meuldijk, A.V. Kyrylyuk, P. van der Schoot, C.E. Koning, Polymer 49 (2008) 2866.
[13] Y. Yang, M.C. Gupta, J.N. Zalameda, W.P. Winfree, Micro Nano Lett. 3 (2008) 35.
[14] A.K. Kota, B.H. Cipriano, D. Powel, S.R. Raghavan, H.A. Bruck, Nanotechnology 18 (2007) 1.
[15] R.B. Mathur, S. Pande, B.P. Singh, T.L. Dhami, Polym. Compos. 29 (2008) 717.
[16] B. Safadi, R. Andrews, E.A. Grulke, J. Appl. Polym. Sci. 84 (2002) 2660.
[17] F.M. Blighe, Y.R. Hernandez, W.J. Blau, J.N. Coleman, Adv. Mater. 19 (2007) 4443.
[18] V. Antonucci, G. Faiella, M. Giordano, L. Nicolais, G. Pepe, Macromol. Symp. 247 (2007) 172.
[19] O. Pekcan, E. Arda, Polym. Int. 49 (2000) 678.
[20] O. Pekcan, E. Arda, V. Bulmus, E. Piskin, J. Appl. Polym. Sci. 77 (2000) 866.
[21] E. Arda, S. Kara, A. Sarac, O. Pekcan, J. Colloid Interface Sci. 297 (2006) 520.
[22] A. Tuncel, R. Kahraman, E. Piskin, J. Appl. Polym. Sci. 50 (1993) 303.
[23] A. Tuncel, R. Kahraman, E. Piskin, J. Appl. Polym. Sci. 51 (1994) 1485.
[24] E. Arda, V. Bulmus, E. Piskin, O. Pekcan, J. Colloid Interface Sci. 213 (1999) 160.
[25] M. Weber, M.R. Kamal, Polym. Compos. 18 (1997) 711.
[26] A.K. Kota, B.H. Cipriano, M.K. Duesterberg, A.L. Gershon, D. Powell, S.R. Raghavan, H.A. Bruck, Macromolecules 40 (2007) 7400.
[27] R. Andrews, D. Jacques, M. Minot, T. Rantell, Macromol. Mater. Eng. 287 (2002) 395.
[28] G. Hu, C. Zhao, S. Zhang, M. Yang, Z. Wang, Polymer 47 (2006) 480.
[29] O. Pekcan, E. Arda, J. Colloid Interface Sci. 20 (2002) 471.
[30] O. Pekcan, S. Ugur, Prog. Colloid Polym. Sci. 128 (2004) 92.
[31] S. Ugur, O. Pekcan, Phase Transitions 78 (2005) 593.
[32] S. Ugur, O. Pekcan, Polymer 4 (2003) 2041.